A Simple Screening Current-Induced Magnetic Field Estimation Method for REBCO Pancake Coils

So Noguchi[1,2], Hiroshi Ueda[3], Seungyong Hahn[4,5], Atsushi Ishiyama[6], Yukikazu Iwasa[2]

[1]Graduate School of Information Science and Technology, Hokkaido University, Sapporo 060-0814, Japan.
[2]Francis Bitter Magnet Laboratory, Plasma Fusion and Science Center, Massachusetts Institute of Technology, MA 02139, USA.
[3]Graduate School of Natural Science and Technology, Okayama University, Okayama 700-8530Japan.
[4]Department of Electrical and Computer Engineering, Seoul National University, Seoul 08826, South Korea.
[5]National High Magnetic Field Laboratory, Florida State University, Tallahassee, FL 32310, USA.
[6]Department of Electrical Engineering and Bioscience, Waseda University, Tokyo 169-8555, Japan.

E-mail: noguchi@ssi.ist.hokudai.ac.jp

Abstract. The development of NMR/MRI $REBa_2Cu_3O_y$ (REBCO, RE = Rare Earth) magnets is undergoing all over the world. However, a screening current-induced magnetic field (SCMF) is a serious problem for NMR/MRI magnets wound with REBCO tapes. The reduction of SCMF is strongly desired, and the estimation of SCMF is also desired at the design stage of REBCO magnets. In order to evaluate a SCMF, a finite element method (FEM) or a boundary integration method is needed so far, and a high-level simulation technique is required.

In this paper, we develop an easy method to estimate a SCMF without any high-level simulation technique. In the developed method, an inductance of a winding turn is calculated and then a screening current is estimated according to the magnetic field penetrating into the winding turn. The SCMF is obtained from the estimated screening current.

The SCMFs computed by the proposed method were compared with measurements and simulation results of the FEM. The results agreed well, but we can see a large difference. However, the SCMFs by the proposed method are enough accurate so that we know the SCMFs at the design stage without using a high-level simulation technique.

1. Introduction

After a No-Insulation (NI) winding technique applying to $REBa_2Cu_3O_y$ (REBCO, RE = rare earth) pancake coils was proposed [1], many institutes have developed REBCO magnets for applications of NMR, MRI, and accelerator [2-4]. However, these magnets may not generate an accurate magnetic field identical to the design values. A major cause is screening currents induced in REBCO tapes by penetrating a magnetic field (Figure 1). An unbalanced current consisting of the transport and screening current generate an undesirable irregular magnetic field. Although screening currents are generated in BSCCO tapes, much larger screening currents are induced in REBCO tape because of a REBCO layer shape. To reduce irregular magnetic fields generated by screening currents, a few methods, e.g. a shaking field effect and an over-shooting charging method, have been shown [5,6]. These methods are effective and useful in the reduction of screening current-induced magnetic field (SCMF), however it is desired to estimate the SCMF at the REBCO magnet design stage.

Many simulation methods of SCMF have also been proposed [4,7-12]. Yanagisawa and Amemiya *et al*. have represented each HTS winding turn with many circular coils, and calculated the screening currents induced in the circular coils [7-9]. Itoh *et al*. have simulated screening currents in REBCO tapes using a 2D finite element method (FEM) and a Biot-Savart law, where a 3D tape structure is transformed into 2D space [10,11]. Ueda *et al*. have obtained screening currents in 3D space using a 3D FEM and the Biot-Savart law accelerated with a fast multipole method in an iteration solver [4,12]. The simulation methods coupling with the FEM and the Biot-Savart law produce an accurate SCMF, however a long computation time and an advanced simulation technique are necessary. The above-mentioned circular-coil-approximation methods also need an approximation technique and a long computation time. Hence, it is desired to develop a simple method to obtain SCMFs. Although the FEM-based method usually takes 1 month, the simple method needs a few ten minutes at the longest.

In the paper, we proposed an easy method to simulate SCMFs and screening currents in REBCO magnets. In the proposed method, the inductance of each turn of REBCO coil is calculated, and then the screening current is obtained from a magnetic field perpendicularly penetrating into REBCO tape surfaces, as shown in Figure 1. Finally, the SCMFs are calculated from the screening currents. The results were compared with measurements and FEM results. Our results showed a qualitative agreement, however small differences can be seen. However, the easily estimated SCMFs are enough accurate to know the characteristics of REBCO magnet. Finally, the inductance of REBCO magnet is given, because a measured inductance is not identical to an ideal one due to screening currents.

2. Simple Screening Current-Induced Magnetic Field Estimation Method

2.1. Screening current-induced magnetic field

Table 1 lists the specifications of a REBCO single pancake coil to derivate the SCMFs. At first, the inductance of REBCO tape with respect to screening current is calculated. As shown in Figure 2, the REBCO single pancake is cut and expanded. When the sheets of expanded REBCO tapes are considered as a coil, the inductance L_{sc} for a screening current is obtained as:

$$L_{\mathrm{sc}} = \frac{\mu_0 N^2 S_{\mathrm{av}}}{d} \quad (1)$$

where μ_0, N, S_{av}, and d are the magnetic permeability of free space, the number of turns, the average area of REBCO tape surface per one turn, and the thickness of REBCO single pancake coil, respectively. When the average magnetic field B_{av} penetrates into the REBCO tapes (as shown in Figure 3), the total magnetic flux Φ is

$$\Phi = B_{\mathrm{av}} wl \quad (2)$$

where w and l are the REBCO tape width and the average length of one turn, respectively. Here, the averaged magnetic field B_{av} is the magnetic field at middle point of cross section of REBCO single pancake coil and easily computed from the Biot-Savart law or the FEM. Hence, as shown in Figure 4, the total induced screening current I_{sc} is derived from:

$$I_{\mathrm{sc}} = \frac{N\Phi}{L_{\mathrm{sc}}} = \frac{B_{\mathrm{av}} d}{\mu_0 N} = \frac{b_{\mathrm{av}} d}{\mu_0 N} I_{\mathrm{op}} = \alpha I_{\mathrm{op}} \quad (3)$$

where $S = wl$ and b_{av} is the average magnetic field per the operating current I_{op} ($B_{\mathrm{av}} = b_{\mathrm{av}} I_{\mathrm{op}}$), and α is the screening current constant, respectively. When a magnet consists of multiple pancake coils connected in serial, the average magnetic field experienced on a pancake coil is given by:

$$B_{\mathrm{av}}^{j} = I_{\mathrm{op}} \sum_{i=1}^{m} b_{\mathrm{av}}^{i}(r_j, z_j) \quad (4)$$

where $B_{av}{}^{j}$, m, and $b_{av}{}^{i}(r_j, z_j)$ are the average magnetic field experienced on the coil j, the number of pancake coils, the average constant of magnetic field generated by the coil i at the location (r_j, z_j) where is at the center of cross section of coil j.

Next, let us derive the magnetic fields generated by the screening currents. Here, we supposed that the screening currents circumferentially flow along the top and bottom edges of REBCO single pancake coil as shown in Figure 5, where the screening currents $I_{sc}{}^{+}$ and $I_{sc}{}^{-}$ are in the opposite direction. That is, screening currents $I_{sc}{}^{+}$ and $I_{sc}{}^{-}$ flows like a circular coil. The magnetic fields B^{+} and B^{-} generated by the circular coils are:

$$B^{+} = \frac{\mu_0}{2} \frac{I_{sc}^{+} r_{av}^{2} N}{\left\{ (h^{+})^2 + r_{av}^{2} \right\}^{\frac{3}{2}}} = \beta^{+} I_{sc} \tag{5}$$

$$B^{-} = \frac{\mu_0}{2} \frac{I_{sc}^{-} r_{av}^{2} N}{\left\{ (h^{-})^2 + r_{av}^{2} \right\}^{\frac{3}{2}}} = -\beta^{-} I_{sc} \tag{6}$$

where h^{+}, h^{-}, r_{av}, β^{+} and β^{-} are the z-position of $I_{sc}{}^{+}$ and $I_{sc}{}^{-}$, the radius of circular coils, and the SCMF constants, respectively.

Finally, we need one assumption that when the coil critical current carries in REBCO single pancake coil, the SCMF becomes zero. Although the screening current phenomenon is much complicated, a linear approximation is employed in the proposed method. As shown in Figure 6, the SCMF linearly decreases with the operating current I_{op} when I_{op} is higher than the half coil critical current (1/2 $I_c{}^{coil}$). Eventually, the SCMF $B_{sc}{}^{sim}$ are represented by:

$$B_{sc}^{sim} = \begin{cases} (\beta^{+} - \beta^{-})\alpha I_{op} & (I_{op} \le \frac{1}{2} I_c^{coil}) \quad \text{(7-a)} \\ -(\beta^{+} - \beta^{-})\alpha (I_{op} - I_c^{coil}) & (I_{op} > \frac{1}{2} I_c^{coil}) \quad \text{(7-b)} \end{cases}.$$

When multiple single or double pancake coils exist, it is possible to obtain the SCMF generated by them according to the superposition principle.

2.2. Coil inductance

The measured inductance of REBCO magnets during charging is smaller than the simulated one, due to the screening current. In this paper, the correction of inductance calculation is shown below.

The magnet constant b_0, which means the on-axis field per operating current, is easily computed using the Biot-Savart law or the FEM. However, the generated on-axis magnetic field is reduced by the screening current. Therefore, the coil inductance L is also reduced by

$$L = \frac{b_0 + b_{sc}^{sim}}{b_0} L_{sim} \tag{8}$$

where L_{sim} is the coil inductance obtained by the simulation, and $b_{sc}{}^{sim}$ is the SCMF constant superposing the SCMF constant of all the pancake coils:

$$b_{sc}^{sim} = \frac{B_{sc}^{sim}}{I_{op}} = \sum_i (\beta_i^{+} - \beta_i^{-})\alpha_i \tag{9}$$

3. Appropriate range of turn-to-turn contact resistivity

To confirm the validity of the proposed simple estimation method, it is applied to two different magnets. The computation results are compared with the measurements and the FEM results. The NI REBCO insert magnet consists of 12 single pancake coils with a radius of 7 mm, and is wound with REBCO tape (SuperPower Inc.) with a REBCO layer thickness of 5 μm.

3.1. 2 double and 4 single pancake coils

At first, the simulation results of the simple estimation method are compared with the SCMF experimental data generated by a magnet, which consists of 2 double and 4 single pancake coils [13] (Figure 7). The specifications of the coils are listed in Table 2. The coils were cooled in a liquid nitrogen bath. The coils were charged in three different conditions; (1) all the pancake coil are simultaneously charged to 30 A with 10 A/min., (2) DPs 1 and 2 and SPs 1 and 2 are charged to 30 A with 10 A/ min., but SPs 3 and 4 are not charged, and (3) SPs 3 and 4 are charged to 30 A with 10 A/ min., but DPs 1 and 2 and SPs 1 and 2 are not charged, as shown in Figure 8. Table 3 shows the experienced magnetic field constants generated by each pancake coil.

In the screening current experiments, the coil constant C_C (T/A) is obtained by measuring a magnetic field with small current applying in the normal state, without screening current. And then, a magnetic field B_0 is measured during charging the coils immersed in liquid nitrogen. Here, the measured screening current-induced magnetic field B_{sc}^{exp} is defined as follows [13]:

$$B_{sc}^{exp}(I_{op}) = B_0(I_{op}) - C_C I_{op} . \quad (10)$$

3.1.1. Case I: All the pancake coils charging at the same time

First of all, all the parameters, the inductance L, the experienced magnetic field constant b_{av}, the screening current constant α, and the SCMF constants β^+ and β^-, of each single pancake coils calculated from (1)-(6) are listed in Table 4.

Figures 9 and 10 show the screening currents I_{sc} and the on-axis SCMFs B_{sc} of each single pancake coil as a function of the operating current I_{op}. Figure 11 presents the simulated SCMF derived from (7) with the experimental data obtained from (8) and the simulation results of the FEM coupled with the thin approximation method (TAM) [14] accelerated by the fast multipole method [15,16]. The peak of the SCMF of the proposed method, the measurement, and the FEM simulation are –1.37 mT at 17.2 A, –0.65 mT at 13.1 A, and –1.49mT at 18.3 A, respectively. The SCMF of the simple estimation method well agreed with that of FEM + TAM, but shows a qualitative agreement with the measurement. Since the SCMF is too small to measure accurately, the quantitative difference would be seen. It can be said that the proposed simple method can easily calculate the screening current-induced magnetic field in a short time (less than 1 s). It took almost 3 days to compute the SCMF by FEM + TAM.

3.1.2. Case II: DPs 1 & 2 and SPs 1 & 2 charging

In this charging pattern, the DPs 1 & 2 and SPs 1 & 2 simultaneously charges to 30 A with 10 A/min., while the SPs 3 & 4 do not charge. However, the screening currents are induced in the SPs 3 & 4 as well as the DPs 1 & 2 and SPs 1 & 2. Since the transport current is zero in the SPs 3 & 4, the screening currents and SCMFs of the SPs 3 & 4 are calculated from (5) and (6) with the average magnetic field contributed by the DPs 1 & 2 and SPs 1 & 2.

The SCMFs of our simple method, the measurements, and the FEM + TAM are given in Figure 12. These three results well agree each other.

3.1.3. Case III: SPs 3 & 4 charging

The SPs 3 & 4 energizes to 30 A with 10 A/min. Although the transport current does not carry into DPs 1 & 2 and SPs 3 & 4, it is necessary to consider the screening currents induced in these coils.

Figure 13 shows the SCMFs of the proposed method, the measurements, and the FEM + TAM as a function of the transport current. The result of our method qualitatively agrees with those of the measurement and the FEM + TAM, and it is smaller than the measurement and the FEM + TAM. However, since the order of these values are identical, the simple estimation method can represent the SCMF well.

Through all the results of cases I-III (Figures 11-13), the absolute value of the SCMF calculated by our method is smaller than that of the FEM + TAM. The causes are: (1) the SCMF is roughly computed using the average magnetic field experienced on pancake coils, and (2) the magnetic fields generated by the screening currents are considered. Nevertheless, the SMCF curves are in good agreement.

3.2. 14-T no-insulation REBCO insert magnet

The proposed simple method to estimate the SMCF is applied to a 14-T no-insulation (NI) REBCO insert magnet which was designed to be inserted into a 31-T LTS outer magnet in order to generate 45 T at National High Magnetic Field Lab., Tallahassee, USA. Figure 14 shows the schematic drawing, and Table 5 indicates the specifications of the insert magnet. To compare the SCMFs, the insert magnet was operated alone in a liquid helium bath, and the on-axis magnetic fields were measured at I_{op} = 9.46 A and 49.8 A. However, since the magnet was wound with the NI technique, the 8.96 A and 48.9 A currents would, respectively, flow in the circumferential direction.

In this experiment, we defined the SCMF as follows. We measured the on-axis magnetic field B_0^{exp}, but it contained the SMCF. Hence, the SCMF B_{sc}^{exp} is derived from subtracting the simulated magnetic field without the SCMF B_0^{sim} from B_0^{exp}:

$$B_{sc}^{exp} = B_0^{exp} - B_0^{sim} \tag{11}$$

The measured SCMF B_{sc}^{exp}, the measured and simulated on-axis magnetic fields are listed in Table 6. Figure 15 plots the measured, proposed, and FEM + TAM simulated SCMFs [11] as a function of transport current. All the SCMFs are in good agreement at the low transport current. The measured SCMF at 48.9 A is higher than the simulated ones, however the order of SCMFs are not largely different.

Figure 16 shows the SCMFs generated by each single pancake. All the SCMFs agree well each other except SPs 6 and 7. The SCMF of SPs 6 and 7 obtained by the simple estimation method are lower than those of the FEM + TAM, because the magnetic fields generated by the screening current in the other SPs are not considered in the proposed method. In addition, the proposed method cannot express the saturation accurately. Although some SCMFs of the FEM + TAM begin saturating between 30 – 40 A, all the SCMFs of our method decrease monotonously.

Next, Table 7 shows the magnet inductances. The measured inductance is low, as compared with the one simulated by FEM. It is caused by the screening current. Hence, the modified inductance is calculated using (8), and it is in agreement with the measured one. It is useful and effective that the inductance can be estimated using the simulation before it is experimentally obtained.

4. Conclusion

Although methods to calculate screening current-induced magnetic fields in REBCO pancake coils have been proposed, high expertise in numerical simulation is required. We propose a new simple calculation method of screening currents and its induced field. In the simple SCMF estimation method, the inductances of REBCO pancake coils on screening current are derived, and then the screening currents induced by the magnetic fields perpendicular to the wide surface of REBCO tape are obtained. Subsequently, the SCMFs are conducted from the screening currents. All the derivation is simple and easy, so it is easy to calculate the SCMFs without high skills in numerical simulation.

Using the proposed method, the SCMFs of a simple magnet consisting of 8 pancake coils are computed and compared with the measurements and the simulation results of the finite element method with the thin approximation method. Although the measurements would be not accurate, both the simulation results are in good agreement. Next, the SCMFs of 12 pancake coils are simulated with the proposed method. The simulated SCMFs agree with the FEM + TAM well, however the measured SCMF is higher than the simulation results. It is hard to accurately measure the SCMFs. This method can deliver the screening current-induced magnetic fields with moderate accuracy, without high expertise in numerical simulation.

Acknowledgement

This work was supported in part by JSPS KAKENHI Grant Number 15KK0192.

Reference

[1] Hahn S, Park D K, Bascuñán J and Iwasa Y 2011 HTS pancake coils without turn-to-turn insulation *IEEE Trans. Appl. Supercond.* **21** 1592–5

[2] Bascuñán J, Hahn S, Kim Y and Iwasa Y 2013 A new high-temperature superconducting (HTS) 700-MHz insert magnet for a 1.3 G-Hz LTS/HTS NMR magnet *IEEE Trans. Appl. Supercond.* **23** 4400304

[3] Miyazaki H, Iwai S, Otani Y, Takahashi M, Tosaka T, Tasaki K, Nomura S, Kurusu T, Ueda H, Noguchi S, Ishiyama A, Urayama S and Fukuyama H 2016 Design of a conduction-cooled 9.4T REBCO magnet for whole-body MRI systems *Supercond. Sci. Technol.* **29** 104001

[4] Ueda H, Fukuda M, Hatanaka, Wang T, Ishiyama A and Noguchi S 2013 Spatial and temporal behaviour of magnetic field distribution due to shielding current in HTS coil for cyclotron application *IEEE Trans. Appl. Supercond.* **23** 4100805

[5] Kajikawa K and Okabe Y 2016 Reduction of screening-current-induced fields in an HTS tape winding using toroidal arrangement of shaking coil *IEEE Trans. Appl. Supercond.* **26** 4400504

[6] Miyazaki H, Iwai S, Uto T, Otani Y, Takahashi M, Tosaka T, Tasaki K, Nomura S, Kurusu T, Ueda H, Noguchi S, Ishiyama A, Urayama S and Fukuyama H 2017 Screening-current-induced magnetic field of conduction-cooled HTS magnets wound with REBCO-coated Conductors *IEEE Trans. Appl. Supercond.* **27** 4701705

[7] Yanagisawa Y, Nakagome H, Koyama Y, Hu R, Takao T, Hamada M, Kiyoshi T, Takahashi M and Maeda H 2009 Effect of current sweep reversal on the magnetic field stability for a Bi-2223 superconducting solenoid *Phys. C, Supercond.* **469** 1996–4

[8] Yanagisawa Y, Nakagome H, Uglietti D, Kiyoshi T, Hu R, Takematsu T, Takao T, Takahashi M and Maeda H 2010 Effect of YBCO-coil shape on the screening current-induced magnetic field intensity *IEEE Trans. Appl. Supercond.* **20** 744–4

[9] Amemiya N and Akachi K 2008 Magnetic field generated by shielding current in high Tc superconducting coils for NMR magnets *Supercond. Sci. Technol.* **21** 095001

[10] Itoh R, Oga Y, Noguchi S, Igarashi H and Ueda H 2013 Numerical simulation of screening current distribution in HTS tape of high field magnet *Phys. C, Supercond.* **484** 300–5

[11] Itoh R, Oga Y, Noguchi S and Igarashi H 2013 Screening current simulation inside YBCO tape in charging YBCO magnet *IEEE Trans. Appl. Supercond.* **23** 4600905

[12] Ueda H, Fukuda M, Hatanaka K, Michitsuji K, Karino H, Wang T, Wang X, Ishiyama A, Noguchi S, Yanagisawa Y and Maeda H 2014 Measurement and simulation of magnetic field generated by screening currents in HTS coil *IEEE Trans. Appl. Supercond.* **24** 4701505

[13] Ueda H, Ishiyama A, Ariya Y, Wang T, Wang X, Agatsuma K, Miyazaki H, Tosaka T, Nomura S, Kurusu T, Urayama S and Fukuyama H 2015 Evaluation of magnetic-field distribution by screening current in multiple REBCO coils *IEEE Trans. Appl. Supercond.* **25** 4700705

[14] Tsuboi H and Kunisue K 1991 Eddy current analysis of thin plates taking account of the source current distributions and its experimental verifications *IEEE Trans. Magn.* **27** 4020–4

[15] Hamada S and Takuma T 2003 Effective preconditioning technique to solve a full linear system for the fast multipole method *IEEE Trans. Magn.* **39** 1666–4

[16] Greengard L and Rokhlin V 1997 A new version of the fast multipole method for the Laplace equation in three dimensions *Acta Numer.* **6** 229–41

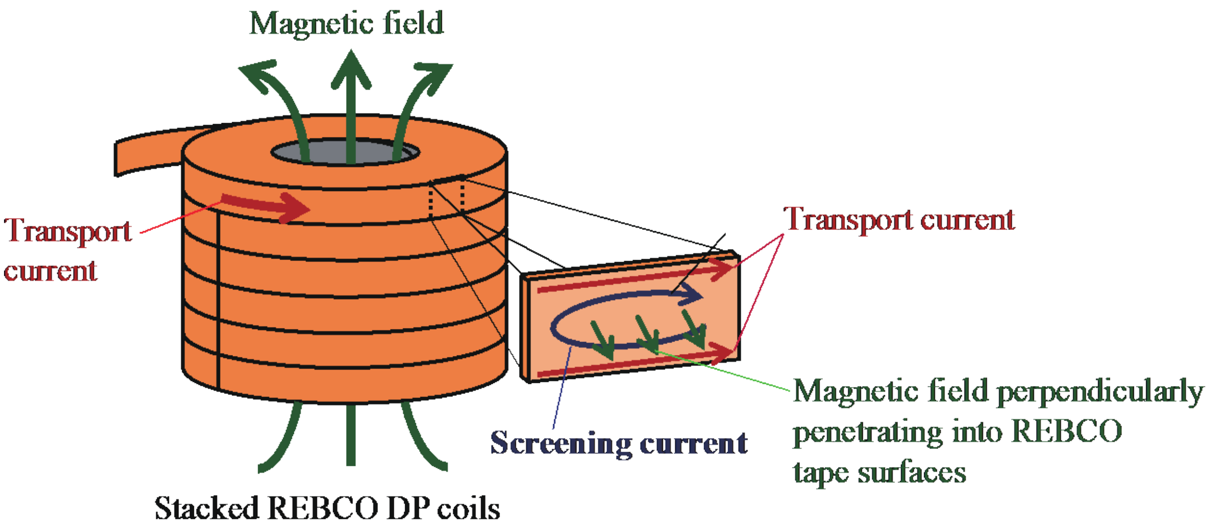

Figure 1. Screening current is induced by magnetic field perpendicularly penetrating into REBCO tape surface.

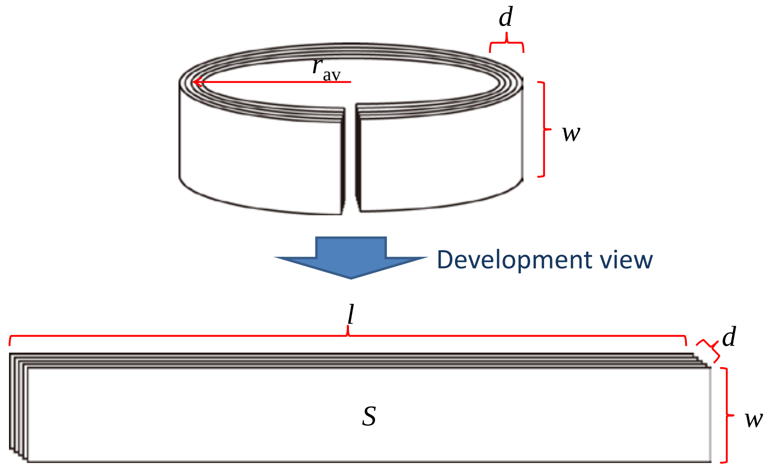

Figure 2. REBCO single pancake coils with parameters, and development view.

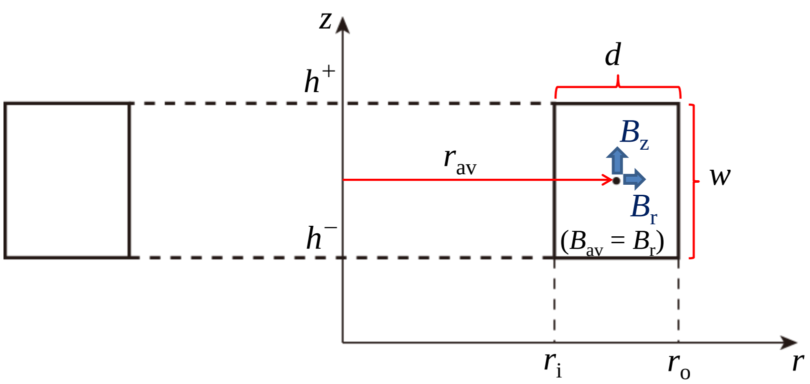

Figure 3. Average magnetic field penetrating into REBCO tape is defined as the r-component of magnetic field at center of coil cross section ($B_{av} = B_r$).

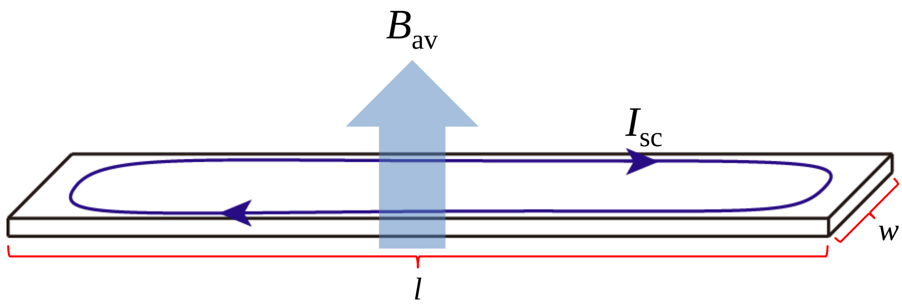

Figure 4. Average magnetic field B_{av} is penetrating into the development coil, and screening current I_{sc} is induced in REBCO tape.

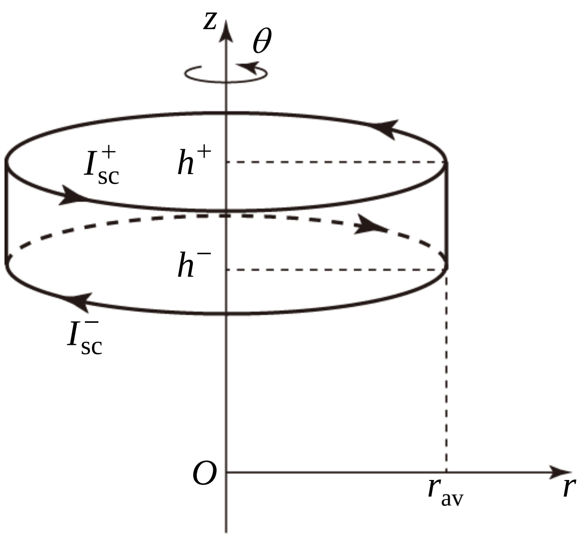

Figure 5. Assuming screening currents I_{sc}^{+} and I_{sc}^{-} flow along the top and bottom edges of coil with average radius of ρ_{av}.

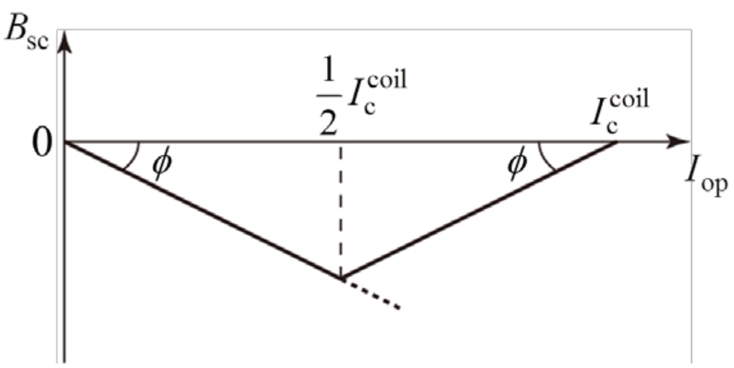

Figure 6. Assuming the screening current-induced magnetic field linearly decreases when the operating current exceeds the half coil critical current.

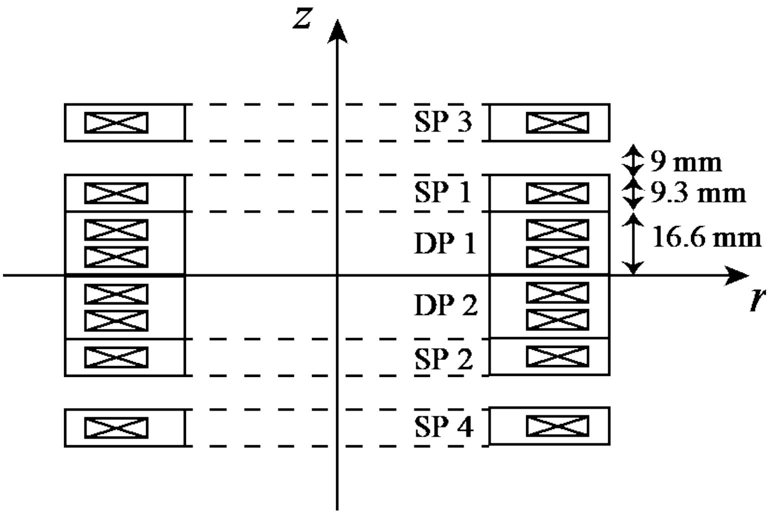

Figure 7. Schematic drawing of the 2 DP + 4 SP coil.

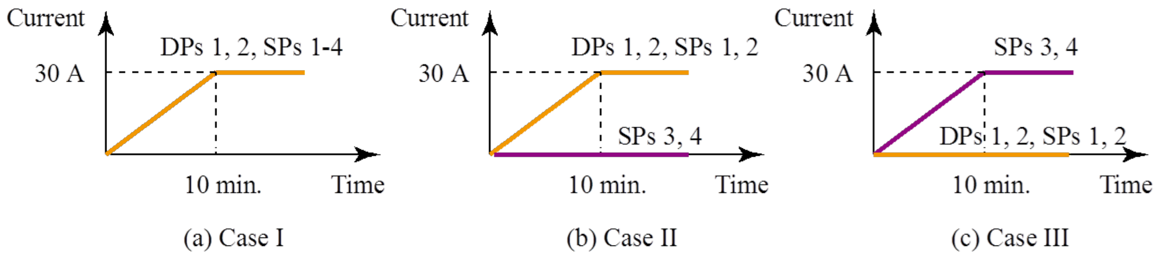

Figure 8. Three different charging cases.

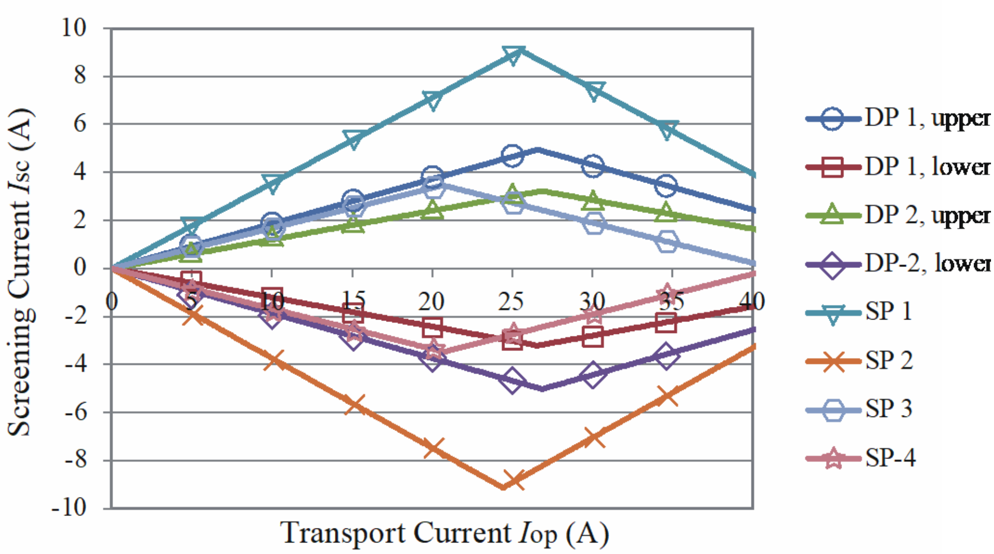

Figure 9. Screening currents of each single pancake coil in case I. The positive direction means the same as the direction of transport current.

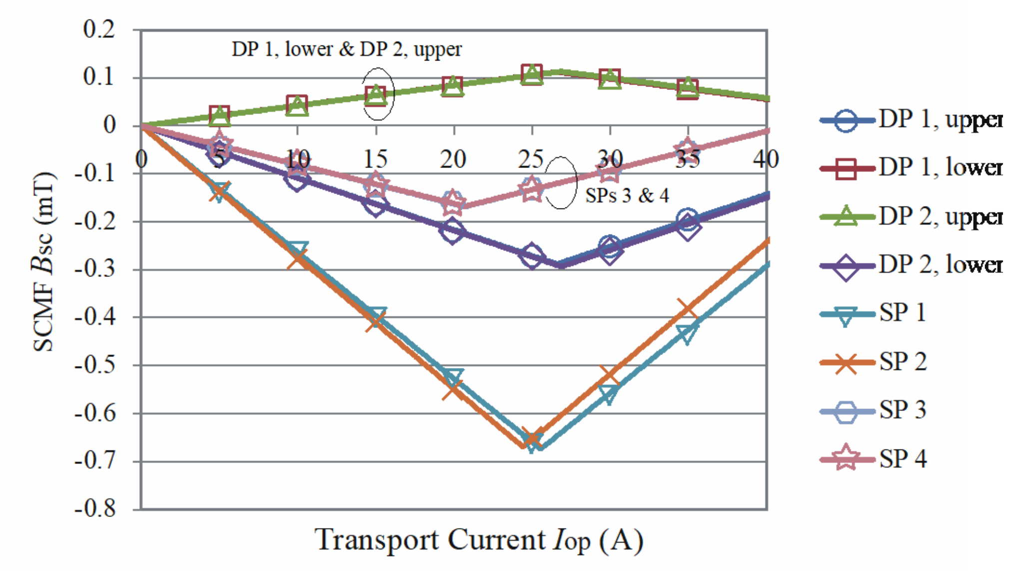

Figure 10. Screening current-induced magnetic field of each single pancake coil in case I.

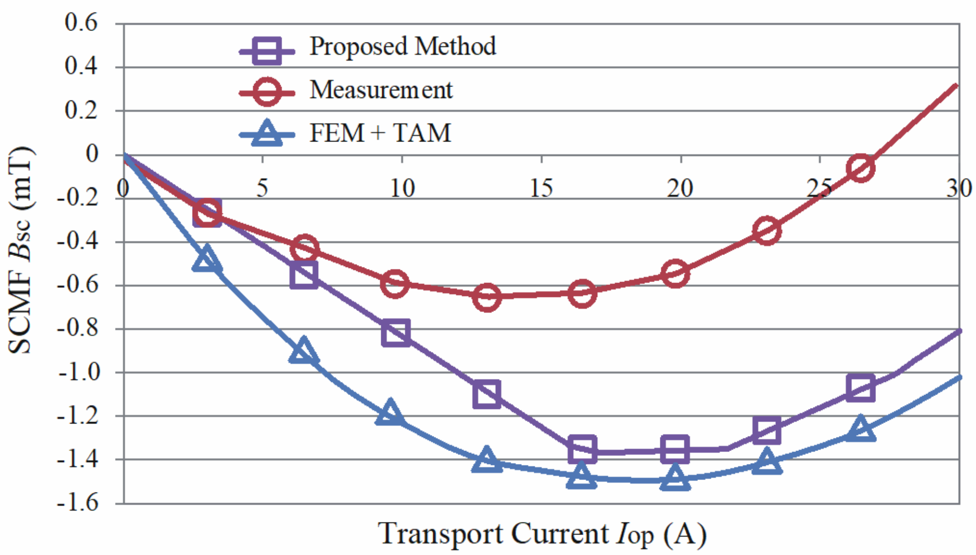

Figure 11. On-axis screening current-induced magnetic fields of the proposed method, measurement, and FEM + TAM in case I.

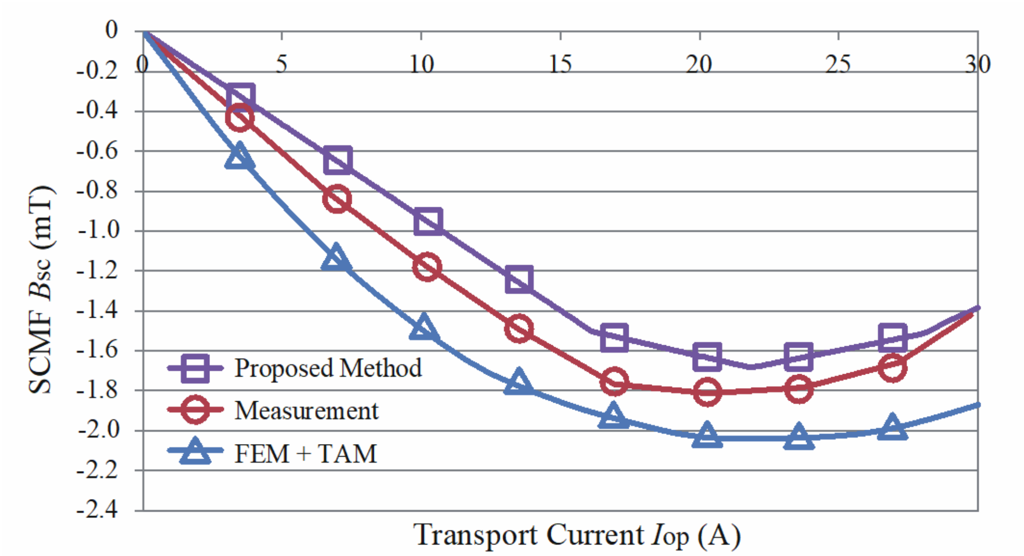

Figure 12. On-axis screening current-induced magnetic fields of the proposed method, measurement, and FEM + TAM in case II.

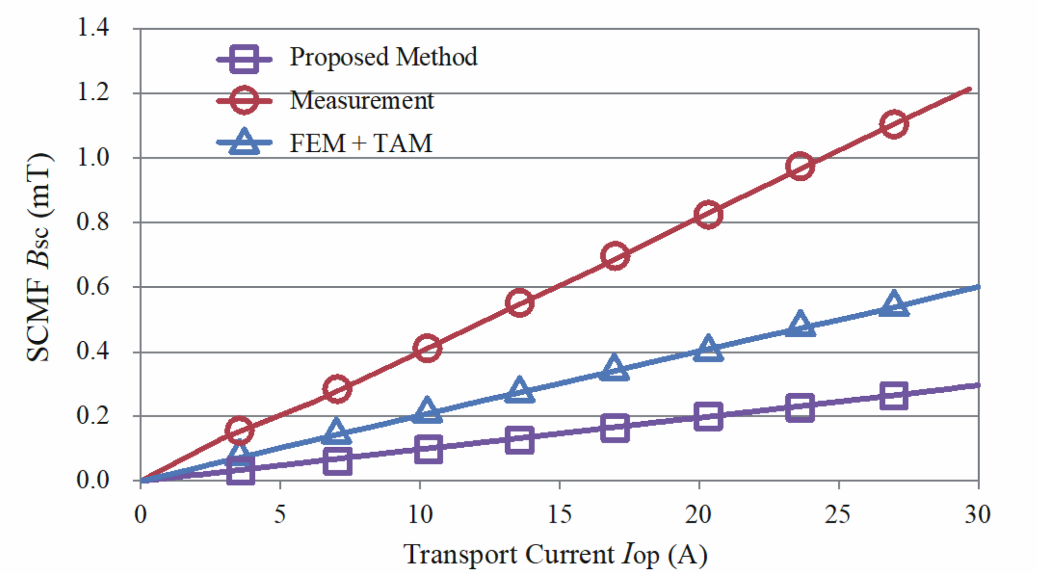

Figure 13. On-axis screening current-induced magnetic fields of the proposed method, measurement, and FEM + TAM in case III.

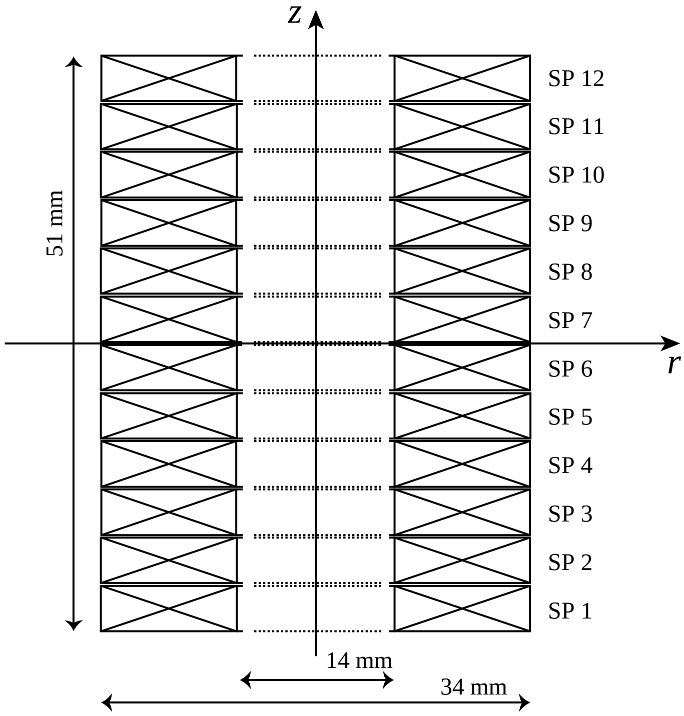

Figure 14. Schematic drawing of the 14-T No-Insulation REBCO insert magnet.

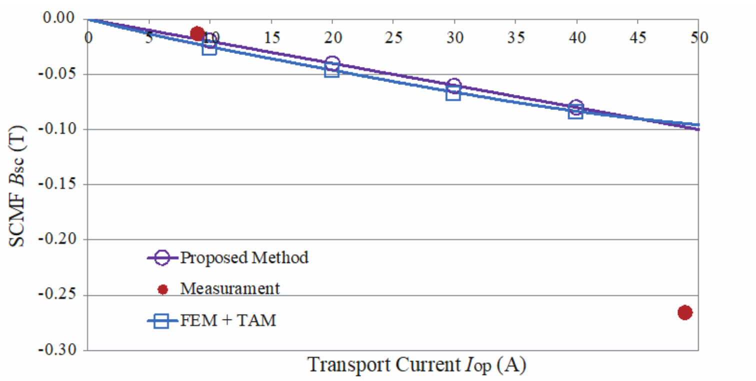

Figure 15. On-axis screening current-induced magnetic fields of the proposed method, measurement, and FEM + TAM by 14-T No-Insulation REBCO insert magnet.

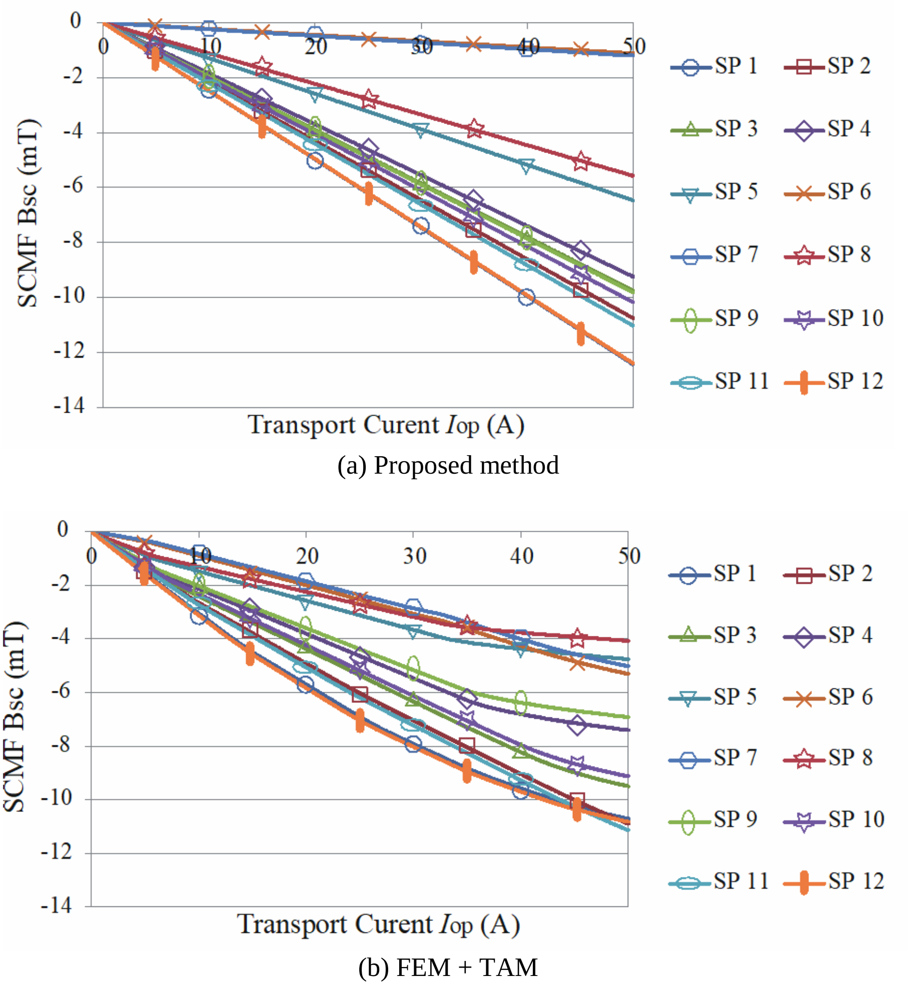

Figure 16. On-axis screening current-induced magnetic fields by each pancake coil by (a) the proposed method and (b) FEM + TAM.

Table 1. Specifications on REBCO single pancake coil

Symbol	Quantity	Unit
ρ_{av}	Average radius of REBCO coil	m
w	Width of REBCO tape	m
d	Thickness of REBCO coil	m
N	Number of turns	Turn
S	Average area of REBCO tape per one turn	m^2
l	Average length of REBCO tape per one turn	m
B_{av}	Average magnetic field penetrating into REBCO tape surface	T
I_{sc}	Screening current	A
h^+	z-position of top of REBCO coil	m
h^-	z-position of bottom of REBCO coil	m
I_c^{coil}	Coil critical current	A
b_0	Magnet constant	T/A

Table 2. Specifications on 2 DP & 4 SP magnet

	DP 1	DP 2	SP 1	SP 2	SP 3	SP 4
Superconducting tape	SuperPower Inc. SCS4050-AP					
Tape width w (mm)	4.0	4.0	4.0	4.0	4.0	4.0
Tape thickness (mm)	0.1	0.1	0.1	0.1	0.1	0.1
Inner radius r_i (mm)	50.0	50.0	50.0	50.0	50.0	50.0
Outer radius r_o (mm)	63.8	63.6	62.8	63.4	63.0	62.9
Average radius r_{av} (mm)	56.9	56.8	56.4	56.7	56.5	56.5
Coil thickness d (mm)	13.8	13.6	12.8	13.4	13.0	12.9
Height (mm)	16.5	16.5	9.3	9.3	9.3	9.3
Average area of REBCO tape per one turn S (mm^2) (each single pancake)	1429	1428	1417	1425	1420	1419
Average length of REBCO tape per one turn l (mm) (each single pancake)	357	357	354	356	355	355
Insulation	Winding with Kapton® 25μm					
Impregnation	No impregnation					
Number of turns N (turn) (each single pancake)	110	110	111	111	111	110
Coil I_c (A) at 77 K, s.f.	118.0	119.9	91.0	64.4	65.0	65.1
Coil I_c^{coil} (A) at 77 K, s.f.	53.17	53.73	51.10	48.86	41.35	41.41
n-value	26.05	28.80	23.46	23.11	22.04	25.43

Table 3. Average magnetic field constants generated by each coil

		DP 1	DP 2	SP 1	SP 2	SP 3	SP 4
DP 1	Upper SP	2.41	1.36	–2.03	0.39	–0.40	0.15
	Lower SP	–2.41	1.98	–1.18	0.52	–0.31	0.18
DP 2	Upper SP	–1.98	2.42	–0.52	1.18	–0.18	0.31
	Lower SP	–1.36	–2.42	–0.39	2.01	–0.15	0.40
SP 1		3.17	0.91	0.00	0.28	–0.59	0.11
SP 2		–0.91	–3.17	–0.28	0.00	–0.11	0.58
SP 3		0.71	0.33	0.59	0.11	0.00	0.05
SP 4		–0.33	–0.71	–0.11	–0.59	–0.05	0.00

Table 4. Parameters to calculate SMCF

		L (mH)	b_{av} (mT/A)	α	β^+ (mT/A)	β^- (mT/A)
DP 1	Upper SP	1.60	1.88	0.186	1.07	1.13
	Lower SP	1.60	–1.22	–0.121	1.16	1.12
DP 2	Upper SP	1.61	1.23	0.120	1.20	1.17
	Lower SP	1.61	–1.91	–0.187	1.13	1.07
SP 1		1.72	3.89	0.355	0.91	0.99
SP 2		1.65	–3.90	–0.374	0.99	0.91
SP 3		1.69	1.80	0.168	0.43	0.48
SP 4		1.67	–1.80	–0.168	0.48	0.43

Table 5. Specifications on 14-T REBCO insert magnet

SP No.	1	2	3	4	5	6	7	8	9	10	11	12
Tape width w (mm)	4.03											
Tape thickness (mm)	0.045											
Inner radius r_i (mm)	7.0	7.0	7.0	7.0	7.0	7.0	7.0	7.0	7.0	7.0	7.0	7.0
Outer radius r_o (mm)	17.0	17.0	17.0	17.0	17.0	17.0	17.0	17.0	17.0	17.0	17.0	17.0
Average radius r_{av} (mm)	12.0	12.0	12.0	12.0	12.0	12.0	12.0	12.0	12.0	12.0	12.0	12.0
Coil thickness d (mm)	5.0	5.0	5.0	5.0	5.0	5.0	5.0	5.0	5.0	5.0	5.0	5.0
Height (mm)	4.03	4.03	4.03	4.03	4.03	4.03	4.03	4.03	4.03	4.03	4.03	4.03
Average area of REBCO tape per one turn S (mm^2)	304	304	304	303	304	304	304	304	303	304	304	303
Average length of REBCO tape per one turn l (mm)	75.4	75.4	75.3	75.3	75.5	75.5	75.4	75.4	75.3	75.4	75.4	75.3
Insulation	No insulation											
Impregnation	No impregnation											
No. of turns N (turn)	231	220	219	217	220	219	219	219	220	219	231	224

Table 6. Measured and simulated on-axis magnetic fields and SCMFs

Current I_{op} (A)	Measured field B_0^{exp} (T)	Simulated field B_0^{sim} (T)	Measured SCMF B_{sc}^{exp} (T)	Proposed SCMF B_{sc}^{sim} (T)	FEM+TAM SCMF B_{sc}^{FEM} (T)
8.96	0.51	0.52	–0.013	–0.018	–0.023
48.9	2.59	2.86	–0.266	–0.098	–0.095

Table 7. Magnet inductances and constants

Simulated inductance L_{sim} (mH)	Measured inductance L_{exp} (mH)	Magnet constant b_0 (mT/A)	SCMF constant b_{sc}^{sim} (mT/A)	Inductance L (mH) corrected by (8)
48.3	46.6	58.4	–2.0	46.6